

A method to measure prompt fission neutron spectrum using gamma multiplicity tagging



E. Blain*, A. Daskalakis, R.C. Block, D. Barry, Y. Danon

Gaerttner LINAC Center, Rensselaer Polytechnic Institute, Troy, NY 12180, USA

ARTICLE INFO

Available online 11 September 2015

Keywords:

Fission
Spectrum
Measurement

ABSTRACT

In order to improve on current prompt fission neutron spectrum measurements, a gamma multiplicity tagging method was developed at the Rensselaer Polytechnic Institute Gaerttner Linear Accelerator Center. This method involves using a coincidence requirement on an array of BaF₂ gamma detectors to determine the timing of a fission event. This allows for much larger fission samples to be used due to the higher penetrability of gammas compared to fission fragments. Additionally, since the method relies on gammas as opposed to fission fragments, the effects of the low level discriminator, used in fission chambers to eliminate alpha events, are not seen. A ²⁵²Cf fission chamber was constructed in order to determine the viability of this method as well as the efficiency when compared to a fission chamber. The implemented multiple gamma tagging method was found to accurately reproduce the prompt fission neutron spectrum for the spontaneous fission of ²⁵²Cf and to detect 30% of fission events.

© 2015 Elsevier B.V. All rights reserved.

1. Introduction

Accurate nuclear data are important for reducing the uncertainty of nuclear simulation codes such as Monte Carlo N Particle (MCNP) [1] and GEANT [2]. These codes require cross-sections and other nuclear data such as energy spectrum for prompt fission neutron emission in order to simulate nuclear processes. This data comes from evaluated nuclear data libraries such as the Evaluated Nuclear Data File (ENDF) [3], the Joint European Fission Fusion (JEFF) [4] evaluation, and the Japanese Evaluated Nuclear Data Library (JENDL) [5]. These evaluated nuclear data libraries combine experimental results with theoretical calculations in order to best determine the value for the nuclear data. Fig. 1 shows several experimental datasets for the prompt fission neutron spectrum (PFNS) for thermal neutron induced fission of ²³⁵U as well as the evaluations from ENDF, JEFF and JENDL. This shows that there is very little experimental data for the PFNS for ²³⁵U particularly in the region below 0.5 MeV. Additionally, the existing data often have large associated experimental errors and, after proper normalization, the shapes do not agree with the evaluated nuclear data libraries. As seen in Fig. 1 all three evaluations are lower than the experimental data in the region below 0.5 MeV. Therefore, more accurate measurements are needed, particularly in the

energy region below 0.5 MeV, in order to more accurately represent the PFNS in simulation codes.

One of the limitations to current PFNS measurements is the mass of fissionable material which can be used in the measurements. Typical PFNS measurements are performed using a fission chamber to determine when a fission event has occurred. These chambers are advantageous due to high efficiency for detecting fission; however, they are limited by the total mass of fissionable material they contain. Conventional fission chambers utilize the energy deposition of fission fragments in a gas volume to determine when a fission event has occurred. Due to the limited range of fission fragments in material, on the order of microns, the fission samples are required to be very thin to allow the fragments to escape the sample [6]. This limits the fissionable mass available in the experiment. Advanced multi-plate fission chambers such as the Parallel Plate Avalanche Counter (PPAC) chamber used at the Chi-Nu experiment station at Los Alamos National Laboratory (LANL) contains 100 mg of fissionable material which is distributed across 10 sample cells with approximately 10 mg of material per cell [7]. This both complicates the fission chamber and requires time of flight corrections based on the sample's location in the detector. These mass limitations require much longer experimental run times in order to get statistically significant data.

In order to increase the sample mass that can be used for PFNS measurements, the prompt fission gammas can be used as a tag that the fission event has occurred. This has been done previously

* Corresponding author.

E-mail address: blaine2@rpi.edu (E. Blain).

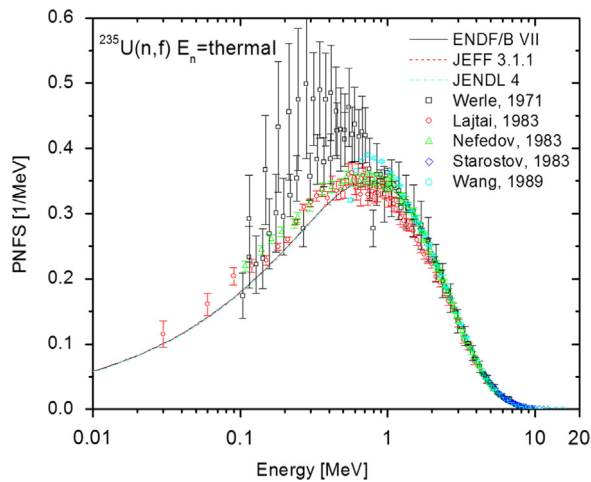


Fig. 1. The PFNS for ^{235}U thermal neutron induced fission showing several relevant datasets as well as the most recent evaluations from ENDF, JEFF and JENDL data libraries.

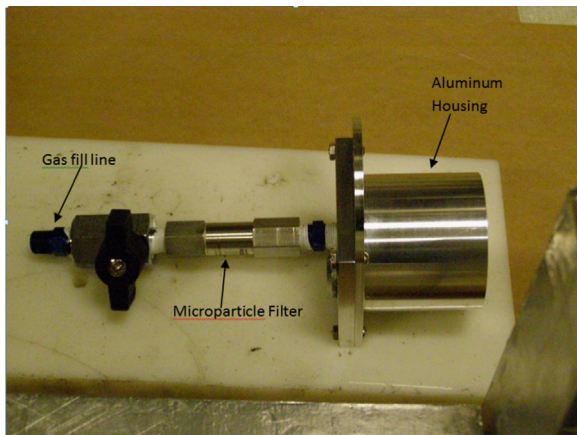


Fig. 2. The ^{252}Cf fission chamber used in the spontaneous fission PFNS measurements. The microparticle filter used to prevent fission fragments from contaminating the gas fill line, along with the gas fill line and aluminum housing are highlighted. The sample plate is located in the center of the aluminum housing.

for PFNS measurements of the spontaneous fission of ^{252}Cf [8]. This method uses any gamma event as the fission start time. While this works well for measurements of spontaneous fission due to the low gamma background rate, it does not work for neutron induced fission where the incident neutron beam provides a large gamma background. Therefore, multiple gamma tagging would be preferable for measurements of neutron induced fission. A multiple gamma tagging technique was previously utilized at the University of Massachusetts Lowell [9]; however, large scattering backgrounds caused difficulties in the measurement. Additionally, gamma tagging has been used to measure the fission cross-section with the gamma multiplicity detector at the Gaertner Linear Accelerator Center at Rensselaer Polytechnic Institute (RPI) [10]. Through the implementation of digital data acquisition, a new multiple gamma tagging method has been developed at RPI in order to measure the PFNS of several isotopes.

2. Gamma tagging method

In order to improve the count rate for prompt fission neutron spectrum measurements, a multiple gamma tagging method was developed at RPI using the RPI neutron scattering system [11]. The gamma tagging method utilizes the high average fission gamma

Table 1

Results from MCNP Polimi modeling for the optimization of the number of gamma detectors used for gamma tagging. The total detection volume was conserved and each detector was modeled as 5 cm thick. Gamma coincidence was used to determine fission and false fission %.

of det.	Det. rad. (cm)	Fiss. %	False fiss. %	FOM
2	7.0	17.3	3.7	4.8
3	5.7	28.3	3.7	7.6
4	4.9	28.7	3.7	7.7
5	4.4	30.9	4.1	7.6
6	4.0	31.4	4.1	7.6
7	3.7	31.3	4.3	7.2
8	3.5	32.5	4.4	7.4

multiplicity, 6.53 for ^{235}U , 6.78 for ^{239}Pu , and 6.95 for ^{252}Cf [12], along with the higher penetrability of gamma rays to allow for much more massive samples to be used. An array of four gamma detectors was oriented next to the fissioning sample, and a coincidence requirement on the array was used to determine when a fission event has occurred. For this application the gamma energy is of little importance, and only the timing of the gamma was required for coincidence. Therefore, BaF_2 detectors were chosen as the gamma detectors of choice, and the timing of the fast detector response component was used for coincidence timing.

Several MCNP Polimi [13] simulations were performed in an attempt to optimize the gamma detector arrangement for the multiple gamma tagging method. For these simulations a ^{235}U sample was placed 10 cm from an array of BaF_2 crystals. A 1 MeV neutron beam was used to induce fission on the ^{235}U sample. Three EJ-301 detectors were modeled as 5 in. diameter by 3 in. thick detectors, which are the size of detectors used currently at the RPI neutron scattering system and located at a distance of 50 cm from the sample. In order to determine which detector configuration was best for the BaF_2 detectors, a figure of merit (FOM) was determined. This FOM is the ratio of the percent of fissions detected with the gamma tagging method over the false fission percent and is given in Eq. (1). The FOM is designed to increase the efficiency of the detection method while limiting the false fission contribution thus a larger FOM is better. The valid fission events are selected by seeing two gammas in coincidence that result from a fission event. The false fission percent is the percentage of events that contain a gamma coincidence of two or greater coming from an event other than fission. This includes events from capture as well as inelastic scattering; however, due to limitation on the simulation, it does not include events from mixed sources such as one gamma from fission and a second from capture. Cross-talk between the detectors was not included in either a valid fission or false fission event in the simulation. A separate simulation was performed in order to quantify this effect. A 1/4 in. lead shield was placed around each detector to limit the cross-talk. The cross-talk between detectors was found to be less than 1% of total fission events.

$$\text{FOM} = \frac{\text{FissionPercent}}{\text{FalseFissionPercent}} \quad (1)$$

The first simulation performed looked at optimization of the number of gamma detectors used for the coincidence measurement. For all gamma detectors in this simulation the thickness of each detector was kept constant at 5 cm. In order to give equal weighting to configurations with different number of detectors, the detector radius was changed for each configuration of detectors in order to preserve the total volume. The results of the MCNP Polimi simulations can be seen in Table 1. Here the FOM is highest for 4 detectors. Although the probability to detect fission is increasing with number of detectors, the FOM is maximized at 4 detectors.

Table 2

Results from MCNP Polimi modeling for the optimization of the gamma detector thickness used for gamma tagging. The simulations involved four detectors with a constant radius of 4.9 cm. Gamma coincidence was used to determine fission and false fission %.

Det. thickness (cm)	Fiss. %	False fiss. %	FOM
1.0	8.0	3.1	2.5
2.0	16.4	2.8	5.8
3.0	22.0	3.1	7.0
4.0	25.5	3.5	7.4
5.0	28.3	3.4	8.4
6.0	30.5	3.5	8.8
7.0	32.3	4.0	8.0
8.0	33.4	4.2	8.0
9.0	34.4	4.2	8.3
10.0	35.0	4.6	7.6

Table 3

Results from MCNP Polimi modeling for the optimization of the gamma detector radius used for gamma tagging. The simulations involved four detectors with a constant thickness of 6.0 cm. Gamma coincidence was used to determine fission and false fission %. The oscillatory behavior at higher detector radii is due to uncertainty in the false fission %.

Det. radius (cm)	Fiss. %	False fiss. %	FOM
4.0	25.2	3.5	7.2
5.0	30.8	3.4	9.2
6.0	34.5	3.4	10.2
7.0	36.8	3.4	10.9
8.0	38.0	3.7	10.3
9.0	39.1	4.0	9.8
10.0	39.1	3.9	10.1
11.0	38.3	3.9	9.8
12.0	38.1	3.8	10.1
13.0	37.4	3.9	9.6
14.0	36.8	4.1	9.0

The second parameter which was optimized was the thickness of the gamma detectors. For these simulations the radius of the detector was constant at 4.9 cm, and four detectors were used which were the previous optimal number of detectors found. The results from the simulations can be seen in Table 2, and an optimal thickness of 6 cm was found.

The final optimization performed was on the gamma detector radius. For these simulations four detectors were used with a thickness of 6 cm as found in the previous optimizations. The results of the simulation can be found in Table 3. This shows that the optimal detector radius is found to be 7 cm. Furthermore, the probability to detect a fission through the multiple gamma tagging method with these parameters is 36.8% with only a 3.4% from false detection. Although the false detection rate seems high, this value was calculated for the probability to get a gamma coincidence from an event other than fission. These events come from capture and inelastic scattering. Since capture reactions do not have a neutron associated with them, any background from these events would be constant and do not greatly affect the measurements. Therefore, only inelastic scattering events would have the gamma coincidence as well as a neutron to be mistaken as fission events. Once this criterion is applied the total false detection rate falls to less than 1% for the given simulation. However, this is dependent on the scattering to fission ratio and therefore will need to be simulated for each measurement.

Through the simulations a final coincidence criterion was obtained. A coincidence of two on an array of four BaF₂ detectors with a coincidence timing of ± 1.5 ns was used. This value for coincidence timing was determined through an experiment looking at the timing resolution of the BaF₂ detectors which is

Table 4

Isotopic composition of ²⁵²Cf sample obtained from ORNL.

Isotope	Atom percent	Weight percent
²⁴⁹ Cf	10.92	10.82
²⁵⁰ Cf	13.68	13.61
²⁵¹ Cf	4.76	4.75
²⁵² Cf	70.64	70.82
²⁵³ Cf	0.00	0.00
²⁵⁴ Cf	0.00	0.00

described in detail later in the paper. A 300 keV energy threshold was chosen to minimize detection of events from radioactive decay gammas. This value was chosen based on the decay gammas of ²⁵²Cf and can be modified based on the decay radiation of the isotope being measured. The timing window for neutron detection from the fission start event was determined to be 600 ns. At a distance of 50 cm this corresponds to a neutron energy of 3.6 keV which is well below the measurement threshold of the neutron detectors. The lowest measurable neutron energy is at 50 keV which corresponds to 162 ns ToF. A thin plastic scintillator was operated at high voltage, 2200 V, to allow for the measurement of low energy neutrons. Since pulse shape discrimination cannot be performed at such low energies another method needed to be employed for gamma neutron discrimination. The majority of gamma events will not be correlated in ToF and therefore will be subtracted as a constant background. The prompt gamma rays from fission are predominantly in the first few nanoseconds after the fission event and are therefore outside the measurement region. A small number of prompt gamma rays will be emitted at longer times due to decay of isomeric states. MCNP Polimi was used to model the effects of these gammas and they were found to contribute less than 0.1%. The timing window sets the limit on the fission rate available to be counted with this method to $5 \cdot 10^6$ fissions per second. This allows for measurement of the complete neutron spectrum while allowing additional time at the end of the measurement window to determine the background coincidence rate. From the simulations this shows that the gamma tagging method is 36.8% efficient at detecting a fission event.

3. Fission chamber

In order to demonstrate that the gamma tagging method could be used to measure the PFNS, a ²⁵²Cf fission chamber was designed and constructed. This allows for the prompt fission neutron spectrum to be measured simultaneously using both the gamma tag as the fission timing signal as well as the signal directly from the fission chamber as the fission timing signal. A 20 ng ²⁵²Cf sample was obtained from Oak Ridge National Laboratory (ORNL) with isotopic distribution give in Table 4. The sample was sent as a powdered sample, which was then dissolved in nitric acid to create a Californium Nitrate solution. Once the solution had evaporated, alcohol was added to the Californium Nitrate, and the sample was deposited onto a titanium sample plate through stippling. Several two microliter depositions were performed on the sample plate resulting in a one inch spot size. The final sample deposition was found to be approximately 18 ng of the original 20 ng corresponding to about 17,000 fissions per second, 99.5% from ²⁵²Cf.

The sample plate was then placed in a parallel plate fission chamber with 2 mm plate spacing between the anode and cathode plates and filled with methane fill gas at 1 atm. The methane fill gas has a high drift mobility which, along with the small plate spacing, facilitates fast signal collection. The plate spacing was also chosen to minimize events seen from alpha decay signals (Fig. 2).

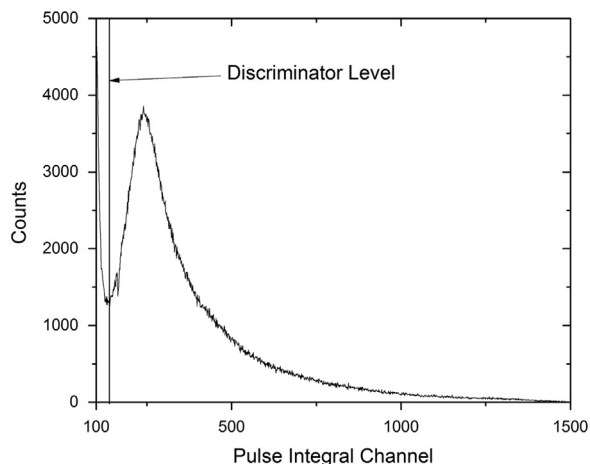


Fig. 3. The pulse integral distribution spectrum for the fission chamber, taken with EAGLE MCA software, showing the alpha peak as well as the fission fragment peak and highlighting the discriminator setpoint chosen to eliminate the alpha signal.

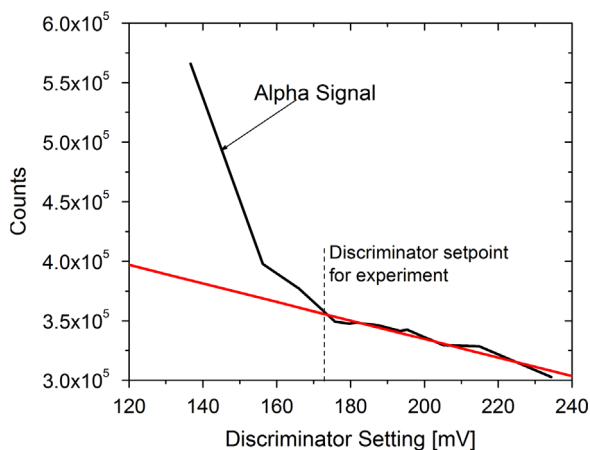


Fig. 4. A measurement of the signal rate from the fission chamber as a function of the discriminator level, taken with Acqiris AP-240 digital data acquisition board, showing the location of the discriminator of alpha fission fragment discrimination and demonstrating the extrapolation method used to determine the detector efficiency.

In order to determine the location of the discriminator as well as the fission chamber efficiency, the fission chamber was connected to an Acqiris AP-240 8 bit 1 Gsample/second digital data acquisition (DAQ) board, and a pulse height spectrum was obtained as seen in Fig. 3. Once the discriminator level had been found, the fission signal was extrapolated back to what it would have been with no discrimination. The ratio of the value at zero discrimination to that at the given discriminator level provides an estimate of the efficiency of the fission chamber, which was found to be 83% efficient as seen in Fig. 4.

4. Experimental setup

The fission chamber was placed on a low mass sample holder in the middle of the RPI neutron scattering system. This system, seen in Fig. 5, utilizes a bank of 4 Acqiris AP-240 DAQ boards to digitally store the detector signals for future post-processing. These boards operate at a Gigasample/second sampling rate resulting in one nanosecond resolution. The detector setup includes an array of gamma detectors that were used for the gamma tagging, as well as neutron detectors, in order to measure

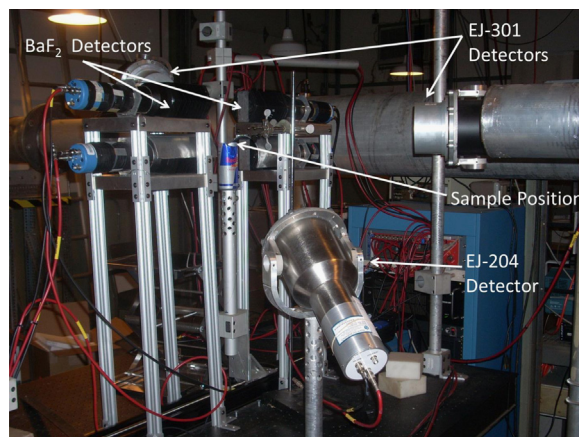


Fig. 5. A figure showing the typical detector setup for a ^{252}Cf spontaneous fission measurement highlighting the location of the gamma detectors, neutron detectors and sample position. An MCNP Polimi simulation was performed to determine the time-dependent neutron background caused by room return from the surrounding materials.

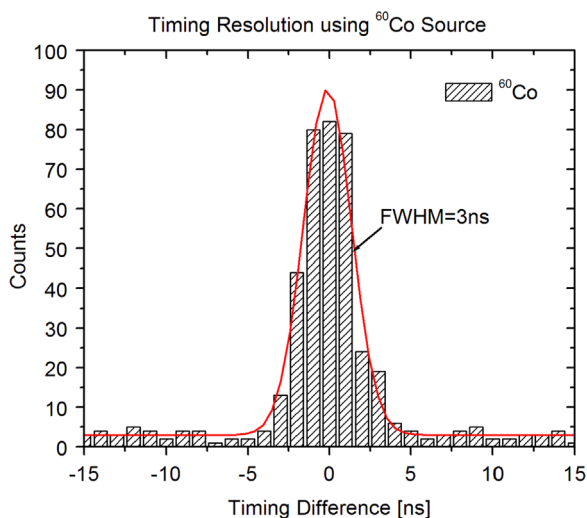


Fig. 6. The timing resolution between 2 BaF_2 detectors found by taking the timing difference between the decay of ^{60}Co . The timing resolution between 2 detectors was found to be 3 ns FWHM and was used as the coincidence timing window.

the prompt fission neutron spectrum. Four BaF_2 gamma detectors were located 10 cm away from the center of the sample plate in the fission chamber. These are hexagonal detectors which were 2 in. across and 5 in. thick. The neutron detectors consisted of two 5 in. diameter by 3 in. thick EJ-301 liquid scintillators for measuring the high energy region (0.5–8 MeV) and one 5 in. diameter by 0.5 in. thick EJ-204 plastic scintillator, that measured the low energy region (50 keV–1 MeV) of the PFNS. The EJ-301 detectors were located 50 cm from the fission source and the EJ-204 detector was located 48 cm from the fission source. This short flight-path will result in a larger uncertainty for the high energy neutrons; however, the system is designed for incident neutron beam measurements and californium is merely used as a benchmark. Increasing the flight-path would result in greatly reduced count rate which will not be useful for incident beam measurements. The uncertainty in the flight-path will be included as an uncertainty in the neutron energy bin. The fission chamber was connected to the DAQ board through an Ortec-142 fast pre-amplifier. All detector signals were recorded with the DAQ boards and post-processed to determine the PFNS.

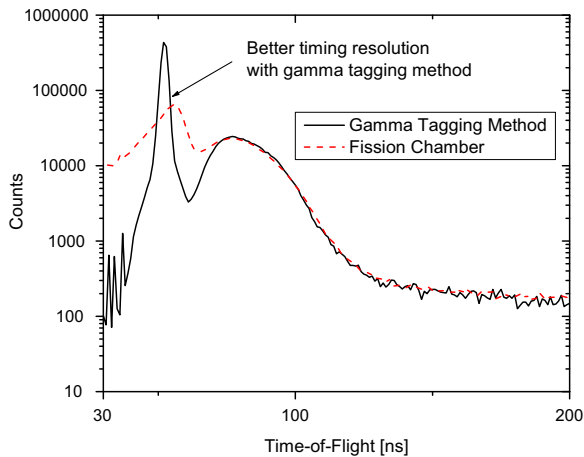


Fig. 7. The PFNS in ToF for the spontaneous fission of ^{252}Cf using both the fission tag from the fission chamber and from the multiple gamma tagging method using an EJ-301 liquid scintillator.

In order to determine an acceptable coincidence timing, the timing resolution of the system had to be obtained. A ^{60}Co source was placed between two BaF_2 detectors, and the timing difference between the signals for each event was recorded. The results of the measurement can be seen in Fig. 6. The measurement was additionally performed for coincidence between the BaF_2 detectors and the EJ-301 and EJ-204 detectors with similar results. This shows that the timing resolution of the system is 3 ns full width half maximum and provides the basis for the coincidence criteria for the gamma tagging method.

5. Results

The prompt fission neutron spectrum was measured using both the signal from the fission chamber and the gamma tag as the start signal. The pulses from the neutron detectors were then recorded for 600 ns after the start signal to provide the full prompt fission neutron spectrum in time of flight (ToF) as well as additional time to provide the constant room background. The ToF results can be seen in Figs. 7 and 8 for an EJ-301 and an EJ-204 neutron detector respectively.

The spectra are aligned based on the centroid of the prompt gamma peak, and the fission chamber was adjusted for the 82% efficiency. The gamma tagging method was then normalized to the fission chamber curve to find the efficiency of the gamma tagging method. This was found to be 30% efficient, which is comparable to the 33.4% efficient found with MCNP Polimi simulations for the current configuration. The PFNS is also comparable using both the fission chamber or the gamma tagging as the start signal. Additionally the results from the gamma tagging method were compared to an MCNP Polimi simulation, using the ^{252}Cf spontaneous fission energy distribution from the Manhart evaluation and a 3 ns Gaussian timing distribution, modeling the detectors and all significant background sources and can be seen in Fig. 9. This shows that the multiple gamma tagging method shows good agreement with the PFNS for ^{252}Cf and can be applied to other materials with larger sample masses than could be used with fission chambers. Lastly, the EJ-204 plastic scintillator was found to behave well in the region below 0.5 MeV down to 50 keV and will be further investigated as a neutron detector for this energy region.

One additional advantage of the gamma tagging method is that it does not rely on the discriminator threshold present in fission chambers. In a fission chamber the detector signal is generated based on the ionization of particles within the fill gas. Both fission

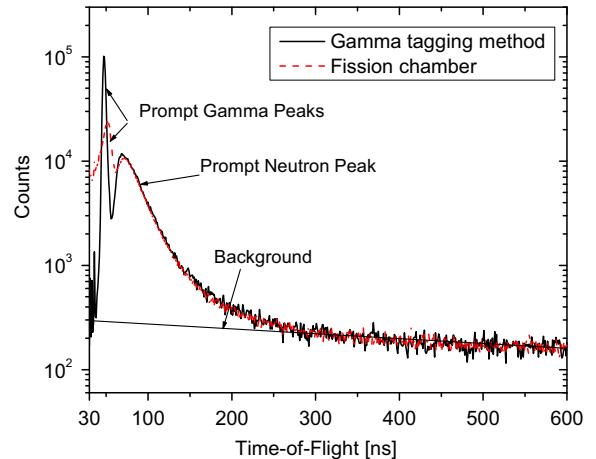


Fig. 8. The PFNS in ToF for the spontaneous fission of ^{252}Cf using both the fission tag from the fission chamber and from the multiple gamma tagging method using a thin EJ-204 plastic scintillator.

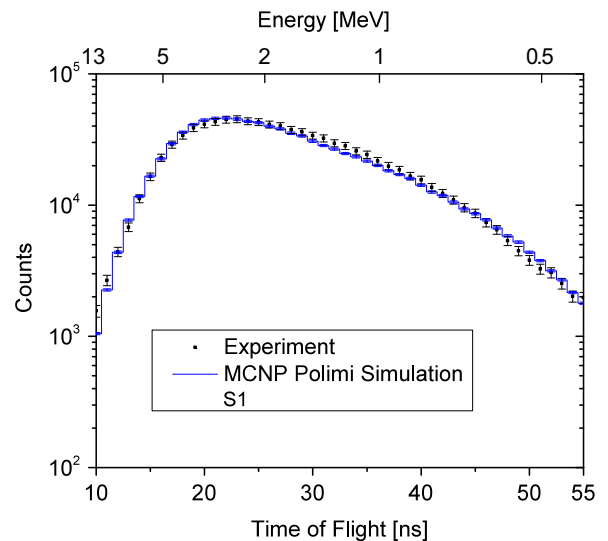


Fig. 9. The PFNS in ToF for the spontaneous fission of ^{252}Cf comparing the experimental data to an MCNP Polimi simulation using the Manhart evaluation energy distribution with a 3 ns Gaussian timing distribution. Although the experiment is higher in the region from 1 to 2 MeV and lower in the region around 0.7 MeV there is good overall agreement between the experiment and simulation.

fragments from fission events as well as alpha particles from radioactive decay cause ionizations in the gas volume. The discriminator is set in order to maximize the number of fission events detected while minimizing the detection of alpha events. The difficulty with this method occurs when the PFNS is measured with a detector parallel to the plates of a parallel plate fission chamber, oriented 90° to the normal of the fission sample, vs. a detector perpendicular to the fission plates, oriented 0° to the normal of the fission sample. A diagram of this configuration can be seen in Fig. 10. Due to the longer ionization path for the perpendicular detector, it will detect more fission events than the parallel detector. Since prompt fission neutrons are preferentially emitted in the direction of the fission fragments [14], this results in slightly different PFNS measured from the parallel and perpendicular detector. In order to demonstrate this effect the ratio of the PFNS for different discriminator setpoints was measured and can be seen in Fig. 10. The discriminator settings were based on maximum pulse height as related to channel on the 8 bit digitizer. How this corresponds to the fission fragment energy deposition spectrum can be seen in Fig. 11. This shows that as the

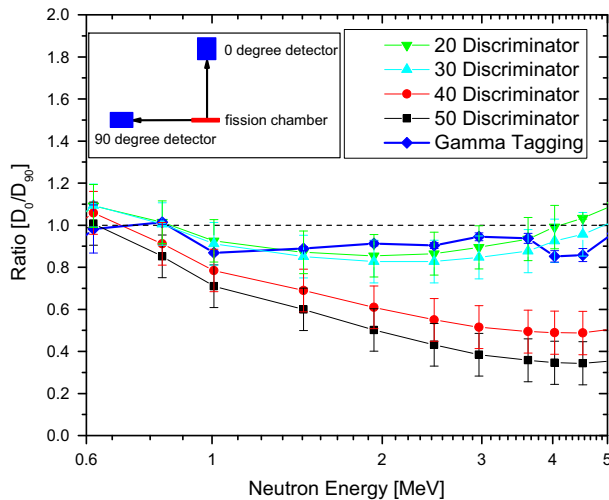


Fig. 10. A measurement showing the effects of the discriminator level on the ratio of the PFNS comparing detectors at 90° and 0° relative to the normal of the parallel plates in the fission chamber and comparing this to the gamma tagging method.

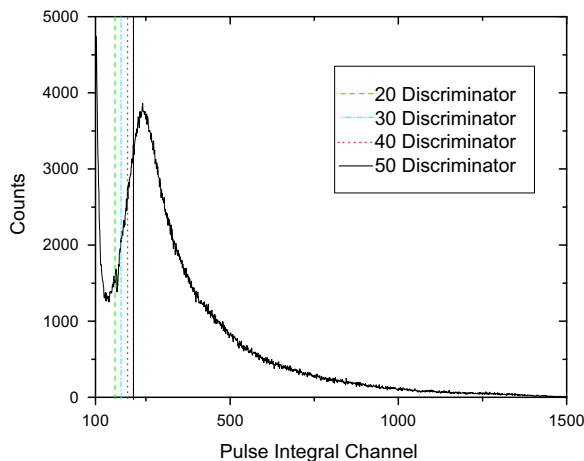


Fig. 11. Where the different discriminator setpoints correspond to the energy deposition of the fission fragments in the fission chamber. The setpoints are based on pulse height in channel on the 8 bit digitizer.

discriminator level increases the PFNS, particularly in the region above 1 MeV, decreases for the parallel detector faster than the perpendicular detector. This phenomenon does not exist for the gamma tagging method since it does not require a discriminator level for fission detection which can be seen in Fig. 10. This demonstrates another advantage of the gamma tagging method over using parallel plate fission chambers.

6. Conclusions

The gamma tagging method has been shown to accurately reproduce the prompt fission neutron spectrum for the

spontaneous fission of ^{252}Cf . The efficiency of the gamma tagging method for the given experimental setup was found to be 30%. Although this is lower than conventional fission chambers, by increasing the mass of the fission sample, the multiple gamma tagging method provides a higher total counting rate over fission chambers. Additionally since it does not require fission fragment neutron discrimination, it does not suffer from the discriminator effects present in current ionization fission chambers. However, when it is used for incident neutron beam measurements, a correction for inelastic scattering must be made. Initial simulations show this correction to be minimal on the order of a few percent and therefore should not limit the use of the gamma tagging method for neutron induced fission measurements. This method can therefore be used to measure the prompt fission neutron spectrum for neutron induced fission on various isotopes of interest including ^{235}U , ^{238}U and ^{239}Pu . Measurements on the full PFNS of ^{252}Cf have already been performed and measurements on the neutron induced fission of ^{238}U are currently being analyzed.

Acknowledgments

The authors express their appreciation to the LINAC staff for their expertise and diligent work. The authors also thank the Stewardship Science Academic Alliance for their funding of this research, Grant numbers: DE-FG52-09NA29453, DE-NA0001814.

References

- [1] MCNP-A General Monte Carlo Code for Neutron and Photon Transport, Version 5, LA-UR-05-8617, Los Alamos National Laboratory, 2005.
- [2] S. Agostinelli, et al., Nuclear Instruments and Methods A 506 (2003) 250.
- [3] M.B. Chadwick, et al., Nuclear Data Sheets 112 (12) (2011) 2887.
- [4] Arjan Koning, et al., Validation of the JEFF-3.1 Nuclear Data Library, JEFF Report 23, 2013.
- [5] K. Shibata, et al., Journal of Nuclear Science and Technology 48 (1) (2011) 1.
- [6] G. Knoll, Radiation Detection and Measurement, third ed., John Wiley and Sons Inc., New York, NY, 2000.
- [7] H.Y. Lee, et al., Prompt fission neutron spectrum study at LANSCE: Chi-Nu Project, Fission and properties of neutron-rich nuclei, in: H. Hamilton Joseph, V. Ramayya Akunuri (Eds.), Proceedings of the Fifth International Conference on ICFN5, World Scientific Publishing Co. Pte. Ltd., Hackensack, NJ, 2014, pp. 430–436.
- [8] S. Naeem, S. Clarke, S. Pozzi, Nuclear Instruments and Methods in Physics Research Section A: Accelerators, Spectrometers, Detectors and Associated Equipment 714 (2013) 98.
- [9] Chuncheng Ji, et al., Measurement of U-235 fission neutron spectra using a multiple gamma coincidence technique, in: AIP Conference Proceedings, vol. 769, 2005, pp. 1051–1053.
- [10] D. Williams, et al., A new method for the measurement of the neutron capture and fission cross sections of ^{235}U , in: Proceedings of the Tenth International Topical Meeting on Nuclear Applications of Accelerators (AccApp 2011), Knoxville, TN, 2011.
- [11] F.J. Saglime, et al., Nuclear Instruments and Methods in Physics Research Section A 620 (2–3) (2010) 401.
- [12] T.E. Valentine, Annals of Nuclear Engineering 28 (2001) 191.
- [13] E. Padovani, S.A. Pozzi, MCNP Polimi User's Manual, 2002.
- [14] N. Kornilov, International Journal of Nuclear Energy Science and Engineering 2 (December (4)) (2012).